Glyphosate-degrading behavior of five bacterial strains isolated from stream biofilms

Florent Rossi, Louis Carles, Florence Donnadieu, Isabelle Batisson, Joan Artigas

Glyphosate-degrading behaviour of five bacterial strains isolated from stream biofilms

Florent Rossi[1], Louis Carles[2], Florence Donnadieu[1], Isabelle Batisson[1] and Joan Artigas[1,*]

1) Université Clermont-Auvergne, CNRS, Laboratoire Microorganismes : Génome et Environnement, F-63000 Clermont-Ferrand, France.
2) Department of Environmental Toxicology (Utox), Swiss Federal Institute of Aquatic Science and Technology (Eawag), Dübendorf, Switzerland.

[*]*Corresponding author*:
Joan Artigas
Laboratoire Microorganismes : Génome et Environnement
1 Impasse Amélie Murat,
TSA 60026, CS 60026
63178 Aubière Cedex, France
Tel : +33 4 73 40 74 73
Fax : +33 473 40 76 70
E-mail: joan.artigas_alejo@uca.fr

Running head: Glyphosate as phosphorus source

Keywords*:* herbicide, AMPA, sarcosine, degradation, C-P lyase, periphyton.

SUMMARY

The present study investigates the individual degrading behaviour of bacterial strains isolated from glyphosate-degrading stream biofilms. In this aim, biofilms were subjected to enrichment experiments using glyphosate or its metabolite AMPA (aminomethyl phosphonic acid) as the sole phosphorus source. Five bacterial strains were isolated and taxonomically affiliated to *Ensifer* sp. CNII15, *Acidovorax* sp. CNI26, *Agrobacterium tumefaciens* CNI28, *Novosphingobium* sp. CNI35 and *Ochrobactrum pituitosum* CNI52. All strains were capable of completely dissipating glyphosate after 125 to 400 h and AMPA after 30 to 120 h, except for *Ensifer* sp. CNII15 that was not able to dissipate glyphosate but entirely dissipated AMPA after 200 h. AMPA dissipation was overall faster than glyphosate dissipation. The five strains degraded AMPA completely since formaldehyde and/or glycine accumulation was observed. During glyphosate degradation, the strain CNI26 used the C-P lyase degradation pathway since sarcosine was quantitatively produced, and C-P lyase gene expression was enhanced 30× compared to the control treatment. However, strains CNI28, CNI35 and CNI52 accumulated both formaldehyde and glycine after glyphosate transformation suggesting that both C-P lyase and/or glyphosate oxidase degradation pathways took place. Our study shows different and complementary glyphosate degradation pathways for bacteria co-existing in stream biofilms.

1. INTRODUCTION

Streams and rivers account for the most impacted ecosystems on the planet since they have been heavily exploited by humans and often used as final receptors of pollution (Meybec 2003). Urbanization, industry, land-use changes and watercourse alterations are the main proximate causes at the origin of river ecosystems changes which results in physical habitats and water chemistry alterations, and shifts in aquatic biodiversity, among other consequences (Malmqvist and Rundle 2002). Alterations in water chemistry have existed for millennia in streams and rivers (Meybeck and Helmer 1989) and the increasing global chemical pollution of surface waters with largely unknown short and long-term effects on aquatic life and on human health is one of the key problems facing humanity (Schwarzenbach *et al.* 2010). Therefore, the necessity of limiting threats of problematic chemicals at their source instead of costly remediation processes have been widely proposed in the scientific literature

(Vörösmarty *et al.* 2010, Schwarzenbach *et al.* 2010) and suggested in national and international policies (Ecophyto II+ 2018, Lamichhane *et al.* 2016, Directive 2009/128/EC). Because biofilms constitute a highly reactive surface area for the sorption and metabolism of contaminants in running waters (Araya *et al.* 2003, Lawrence *et al.* 2001, Tien *et al.* 2013), their study to alleviate specific water pollution problems becomes a potential solution. However, few studies have investigated the natural potential of aquatic biofilms for the removal of chemicals (*e.g.* Wang *et al.* 2016b, Carles *et al.* 2019).

Glyphosate (N-[phosphonomethyl] glycine) has become the most commonly used herbicide worldwide (Benbrook 2016, Duke and Powles 2008) with about 600 to 750 thousand tonnes used annually in the world and an expected 740 to 920 thousand tonnes to be used by 2025 (Maggi *et al.* 2020). The potential of glyphosate retention in topsoil layers is high due to its strong sorption on clay, iron and aluminium oxide particles (Borggaard and Gimsing 2008, Okada *et al.* 2016, Rampazzo *et al.* 2013, Sidoli *et al.* 2016, Vereecken 2005). Consequently, the immediate leaching of aqueous glyphosate residue is relatively low. However, 98 % of residues adsorbed onto these soil minerals are prone to remobilize if specific agricultural practices are applied (i.e. tillage and ploughing in combination with irrigation and soil pH variations, Maggi *et al.* 2020). Yang *et al.* (2015) showed that up to 14 % of applied glyphosate is transported by runoff and suspended load from clay loam soil with a rain intensity of 1 mm/min for 1 h. Therefore, glyphosate and AMPA can reach streams and rivers through chronic and/or peak exposure events, the latter occurring over hours to a few days depending on the intensity and duration of rain events (Daouk *et al.* 2013). Glyphosate and AMPA concentrations during peaks can reach up to hundreds of micrograms per litre, although basal concentrations rarely exceed a few micrograms per litre (Battaglin *et al.* 2014, Carles *et al.* 2019). Also, it must be noted that other sources of AMPA such as detergents, fire retardants, anti-corrosives and anti-scaling agents can enter streams and rivers through wastewater treatment plant effluents (Grandcoin *et al.* 2017, Nowack 2003, Struger *et al.* 2015, Studnik *et al.* 2015). Generalized exposure to glyphosate makes aquatic microbial communities in sediments prone to acquire tolerance (Bonnineau, unpublished data) and develop transformation and/or mineralization capacities in periphyton (Carles *et al.* 2019, Artigas *et al.* 2020).

Glyphosate degradation is essentially driven by microorganisms (Mallat and Barceló, 1998). Up to now, two main biodegradation pathways have been described (Figure 1): i) the glyphosate oxidase pathway (or AMPA pathway), which involves the cleavage of the C-N bond of the glyphosate molecule by glyphosate oxidoreductase or glycine oxidase enzymes

(+FAD), releasing both AMPA and glyoxylate. Glyoxylate is further metabolized into glycine or via the glyoxylate cycle into microbial biomass and carbon dioxide (Borggaard and Gimsing 2008), while AMPA can be degraded by C-P lyase enzymes, releasing inorganic phosphorus and methylamine, the latter being degraded into formaldehyde and incorporated into microbial biomass. And ii) the C-P lyase pathway (or sarcosine pathway), which involves the cleavage of the C-P bond of the glyphosate molecule by C-P lyase enzymes (encoded by the *phn* operon, Hove-Jensen *et al.* 2014), releasing both inorganic phosphate and sarcosine. Sarcosine may further degrade into glycine and formaldehyde by sarcosine oxidase to finally incorporate the microbial biomass. The prevalent glyphosate degradation pathway employed by bacteria is the sarcosine pathway (13 strains) followed by the AMPA pathway (8 strains) and some strains are able to use both AMPA and sarcosine pathways (4 strains) (Zhan *et al*. 2018). In addition, molecular dynamics simulation studies confirmed the stability of the enzyme-substrate complex for glyphosate oxidoreductase and C-P lyase demonstrating that both enzymes could be preferred in glyphosate biodegradation (Bhatt *et al*. 2021).

Figure 1. Glyphosate and AMPA degradation pathways in the environment.

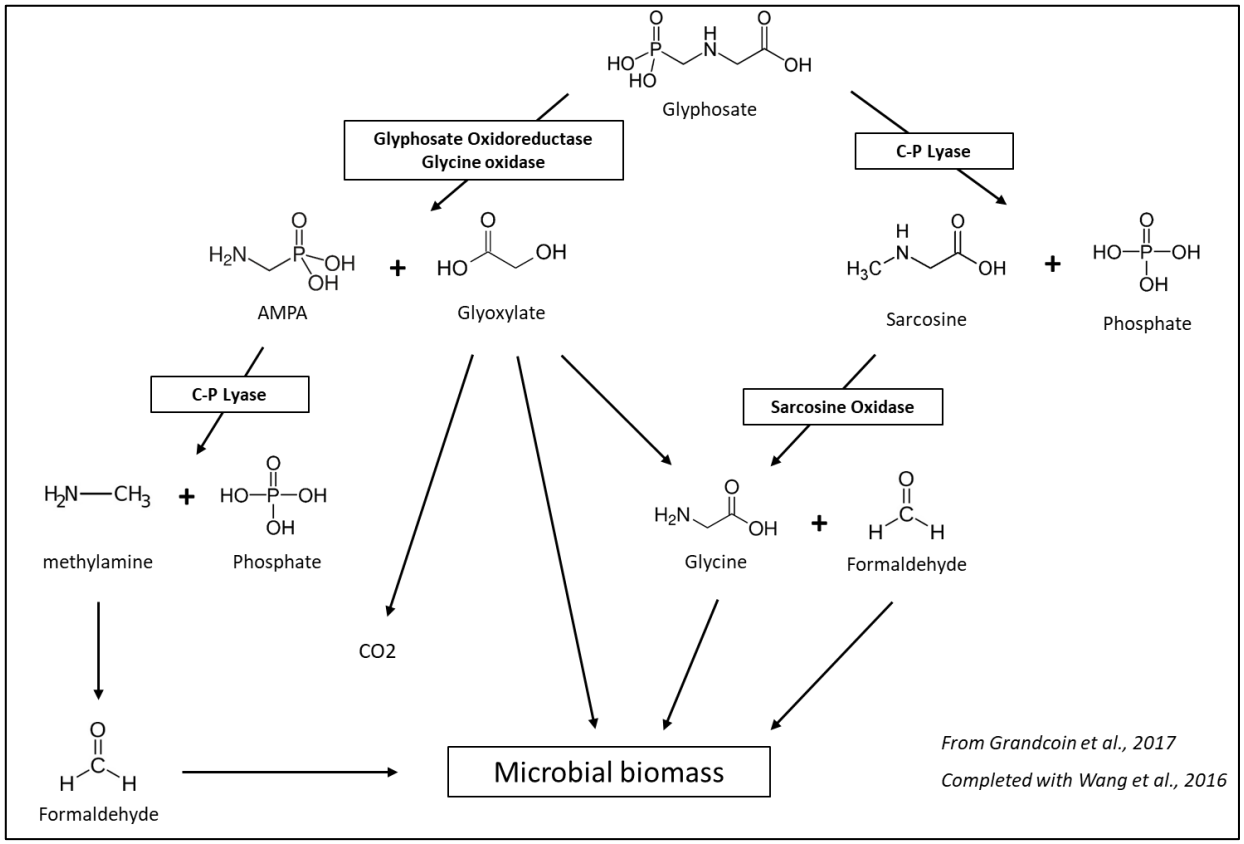

The occurrence of either of these pathways in aquatic systems is still unknown, though projections indicate that the oxidative pathway prevails in soils worldwide (Maggi *et al.* 2020). Up to now, most of the bacterial strains studied are capable to convert glyphosate to AMPA (*Pseudomonas* sp. SG-1 (Talbot *et al.* 1984), *Agrobacterium radiobacter* SW9 (Mcauliffe *et al.* 1990) and *Ochrobactrum anthropi* GPK 3 (Sviridov *et al.* 2012)), even in bacteria that have never been exposed to glyphosate previously, possibly highlighting widespread detoxification mechanisms (Sviridov *et al.* 2015). Furthermore, the C-P bond has been reported to be cleaved by several other strains (*Achromobacter* sp. MPS 12A *(*Sviridov *et al.* 2012) and *Arthrobacter* sp. GLP-1 (Pipke *et al.* 1987)). This highlights the ability of microbes to use both glyphosate and AMPA as a carbon (C) and phosphorus (P) source for their metabolism, although this has been shown to be closely linked with dissolved nutrient availability in water (Carles *et al.* 2019, Hove-Jensen *et al*. 2014, Sviridov *et al*. 2014, Zhang and van der Donk 2012, Bazot and Lebeau 2008). However, it must be noted that most of the knowledge so far comes from bacteria isolated from soils and activated sludge while few studies have investigated glyphosate degradation pathways by bacteria in streams and rivers (Zhan *et al*. 2018, Jacob *et al.* 1988).

In order to improve our knowledge on glyphosate and AMPA biodegradation potential in streams, we used glyphosate-degrading biofilms (Carles *et al.* 2019) in enrichment cultures using glyphosate as the sole P source. Five bacterial strains were isolated and their ability to use glyphosate and AMPA as P source investigated. Each strain was tested separately for glyphosate and AMPA degradation and compared to a control supplemented with K_2HPO_4. Glyphosate and its metabolites (AMPA, sarcosine, formaldehyde and glycine) were analysed during experiments in order to identify the degradation pathway(s) used by each strain. Because our study is the first literature report of an *Acidovorax* sp. strain capable to degrade glyphosate, we focused on the molecular mechanisms of the strain *Acidovorax* CNI26 responsible for glyphosate/AMPA degradation. We first hypothesize faster degradation of AMPA than glyphosate since AMPA is easier to degrade and less toxic for aquatic microorganisms compared to glyphosate. Accordingly, the biomass growth of strains will also be faster with AMPA than glyphosate. Second, the *Acidovorax* CNI26 strain is expected to rapidly overexpress the C-P lyase gene in the presence of AMPA, while overexpression on both C-P lyase and glyphosate oxidase genes can be displayed in the presence of glyphosate. The expression of these two genes will depend on glyphosate and AMPA concentration variation in the media throughout the experiment. The objectives of this study were i) to analyse the glyphosate and AMPA-degrading behaviour of five bacterial strains isolated from

stream biofilms and ii) to investigate the pathway employed by the strain *Acidovorax* CNI26 to degrade glyphosate and AMPA by targeting the C-P lyase and glyphosate oxidase genes.

2. MATERIALS AND METHODS

2.1 Chemicals and media

Glyphosate (N-[phosphonomethyl] glycine (purity ≥ 98 %)), AMPA (aminomethyl phosphonic acid (purity ≥ 99 %)) and K_2HPO_4 (purity ≥ 98 %) were purchased from Sigma Aldrich (France). Acid phenol, TRIzol® and TURBO DNAse were purchased from ThermoFisher Scientific (France). MOPS^{CN} medium (P-free), pH 7.4, was made up of: 40 mM MOPS (3-(N-Morpholino)propanesulfonic acid), 4 mM tricine, 10 µM $FeSO_4$, 276 µM K_2SO_4, 0.5 µM $CaCl_2$, 525 µM $MgCl_2$, 50 mM NaCl, 30 mM $(NH_4)_6Mo_7O_{24}.4H_2O$, 4 µM H_3BO_3, 0.3 µM $CoCl_2.6H_2O$, 0.1 µM $CuSO_4.5H_2O$, 0.8 µM $MnCl_2.4H_2O$, 0.1 µM $ZnSO_4.7H_2O$, 0.3 µM Thiamine HCl, 22 mM Glucose, 9.5 mM NH_4Cl. MOPS^{CN}agar plates were prepared by adding 1.5 % (w/v) agar into the liquid media.

2.2 Enrichment cultures and isolation of bacteria

Glyphosate- and AMPA-enrichment cultures as described by Batisson *et al.* (2009) were run with stream biofilms from Carles *et al.* (2019). From this experiment, we selected river biofilms (namely, Ups_LowP_LowG and Dws_LowP_HighG), having proven their strong capacity to dissipate glyphosate without AMPA accumulation in the media, for subsequent isolation of glyphosate/AMPA-degrading strains. Biofilms were scraped, pooled, and suspended in 2 mL of sterile 0.8 % NaCl solution. Biofilm suspensions were then centrifuged (13,000 *g*, 10 min at 4 °C), and the pellet was washed three times with 2 mL of sterile 0.8 % NaCl solution in order to remove glyphosate or AMPA residues. Biofilm pellets were suspended in 2 mL of sterile 0.8 % NaCl solution and homogenised. This biofilm suspension was used as the inoculum for enrichment cultures.

A volume of 125 µL of each biofilm suspension was added to 12.5 mL of MOPS^{CN} media supplemented with glyphosate (0.5 mM) in 50 mL flasks. Phosphorus contained in the glyphosate molecule was the only source of P in the culture media. Two additional enrichment steps were carried out every 3 weeks by sub-culturing 125 µL of the culture into

12.5 mL of fresh medium containing 2 and 4 mM of glyphosate, respectively. During the enrichment culture steps, the flasks were incubated at room temperature in an orbital shaker at 100 rpm in the dark. The cultures were sampled at the beginning (day 0) and the end (day 21) of each enrichment step to determine glyphosate concentration (see details in section 2.4). At the end of the third enrichment step, cultures were spread for bacterial isolation on $MOPS^{CN}$ agar plates containing the same glyphosate concentrations as in liquid $MOPS^{CN}$ (4 mM). Pure colonies were tested separately for their capacity to transform glyphosate and AMPA in liquid $MOPS^{CN}$ media containing 0.5 mM of glyphosate. Liquid cultures were incubated and sampled for glyphosate and AMPA concentration determination at the same incubation conditions described above. Among the isolates, 5 pure strains degrading glyphosate and/or AMPA in $MOPS^{CN}$ medium were selected for further chemical and molecular characterization.

2.3 Identification and phylogenetic analysis of bacteria

The identification of the 5 strains degrading glyphosate and/or AMPA was carried out by 16S rDNA gene sequencing as described by Batisson *et al.* (2009). The sequences were deposited in GenBank under the accession numbers MN017826, MN017827, MN017828, MN017829 and MN017830, corresponding to isolates CNII15, CNI26, CNI28, CNI35 and CNI52, respectively.

Phylogenetic analysis based on 16S rDNA gene sequences was carried out by multiple alignments (Clustal Ω) followed by the construction of a phylogenetic tree (MEGA 6.0 software). In addition to the 16S rDNA sequences of the 5 newly isolated strains (present study), sequences from previously isolated glyphosate-degrading strains were also included in the analysis. Only one sequence per genus was included in the analysis, either the 16S rDNA gene sequence of the glyphosate-degrading strain described, or the sequence of a corresponding genus/species if the 16S rDNA degrading strain sequence was not available.

2.4 Biodegradation tests with bacteria

The use of glyphosate, AMPA and K_2HPO_4 as P sources by the five strains was determined separately. These strains were inoculated at 10^5 cell mL^{-1} in 120 mL of $MOPS^{CN}$ liquid media supplemented with 0.132 mM of P-equivalents of glyphosate, AMPA or K_2HPO_4 in 225mL

polyethylene flasks. Non-inoculated media served as abiotic controls. Each experiment was carried out in triplicate. The cultures were incubated in the dark at room temperature and 100 rpm agitation for 2 weeks. Six samplings were performed (6 × 1 mL) to monitor strain growth (Optical Density $OD_{\lambda = 600nm}$) and variation in concentrations of glyphosate, AMPA, K_2HPO_4, sarcosine, formaldehyde and glycine over time. The same experiment was repeated later on, in the exact same conditions and 5 mL of culture was recovered to assess gene expression kinetics of C-P lyase and glyphosate oxidase in the CNI26 strain. All samples were kept frozen at -20 °C before glyphosate and glyphosate-metabolite concentration analysis.

Bacterial Abundance: Bacterial abundance during biodegradation tests was estimated in triplicate using a conversion factor obtained from the correspondence curves between optical density at 600 nm and cell counting on flow cytometry. For each of the five bacterial strains, correspondence curves were obtained by following the growth of one colony in 10 mL of $MOPS^{CN}$ liquid media supplemented with 0.132 mM of K_2HPO_4 every 24 hours during one week. Samples were first measured for OD_{600} and then fixed with formaldehyde (2 %, final concentration) before flow cytometry analysis. Twenty-five microliters of fixed bacterial suspension was diluted 10-fold in TE buffer (10 mM Tris, 1 mM EDTA) and stained with 2.5 µL of SYBR Green I before counting bacterial cells with a BD FACSCalibur flow cytometer (15 mW at 488 nm, Becton Dickinson, USA). Correspondences obtained were 1 AU = 5×10^8 cell mL^{-1} for CNI15, 2.8×10^8 cell mL^{-1} for CNI26, 4.2×10^8 cell mL^{-1} for CNI28, 5×10^8 cell mL^{-1} for CNI35 and $8{,}2 \times 10^8$ cell mL^{-1} for CNI52.

Glyphosate and metabolites concentration: Glyphosate and AMPA concentrations were determined in triplicate from 1 mL of culture media following the method of Wang *et al.* (2016a) with some modifications. Briefly, standards of glyphosate and AMPA (0-100 μM) prepared on $MOPS^{CN}$ liquid media and culture samples were derivatized with 9-fluorenylmethylchloroformate (FMOC-CI) and analysed by HPLC (Waters Inc., MA, U.S.A) coupled with a Diode Array Detector (DAD) detector set at λ = 265 nm, and a reverse phase column (Phenomenex Kinetex EVO C18, 5 μm, 150 x 4.6 mm) at 22 °C. The mobile phase was made up of 5 mM ammonium acetate pH 9 (Solvent A) and methanol (Solvent B) at a flow rate of 1 mL min^{-1}, linear gradient 0–5 min: 80 % A; 5–11 min: 80-30 % A; 11–16 min: 30 % A; 16–20 min: 30-80 % A; 20–30 min: 80 % A. Glyphosate and AMPA were detected at 2.8 and 12.4 minutes retention time. Sample taken in triplicate were injected twice. Glyphosate and AMPA quantification in the strain's biomass was measured at the end of experiments following the method described in Carles *et al.* (2019).

Sarcosine, glycine and formaldehyde (MAK073-1KT, MAK261-1KT and MAK131-1KT, respectively) concentrations were determined fluorometrically in triplicate from 1 mL of culture media using assay kits purchased from Sigma Aldrich and following the manufacturer's recommendations. Measurements were performed on a Spark 10M (Tecan, Switzerland) multimode microplate reader. Excitation/emission wavelengths were set up to 535/587 nm for sarcosine and glycine concentration determination and 370/470 nm for formaldehyde concentration determination. Glycine concentration was also determined in K_2HPO_4 and AMPA treatments as background control since glycine is a common metabolite produced by bacteria. The orthophosphate (PO_4^{3-}) concentration was determined in triplicate from 1 mL of culture media using a spectrophotometer (890 nm, Genesys™ 20, ThermoSpectronic, NY, USA) according to the protocol of Murphy and Riley (1962).

C-P lyase and glyphosate oxidase genes in CNI26: The genome of the strain CNI26 was sequenced and the diversity of C-P lyase and glyphosate oxidase genes was analysed to design specific primers for further gene expression experiments. The shotgun genomic library of CNI26 was prepared with the Hyper Library construction kit from Kapa Biosystems (Roche). The library was quantified by qPCR and sequenced on one MiSeq Micro flow cell for 251 cycles from each end of the fragments using a MiSeq 500-cycle sequencing kit version 2. The program used to perform de-novo genome assembly was Spades, version 3.11.1. The size of the assembly was 5.75Mb which means that the approx. genome coverage was 270×. The assembly was fragmented in 89 scaffolds. We took the longest scaffold (700

kb) and compared it to the closest sequences retrieved in GenBank database using BLAST. The top hit was CP003872.1 *Acidovorax sp*. KKS102. The genome assembly was annotated with Prokka v 1.3. Annotation results reveal the presence of one glycine oxidase gene copy and two C-P lyase pathway-encoding operons including genes for: transport proteins (phnCDE), known enzymatic activity in phosphonate catabolism (phnIJMLN), auxiliary polypeptides involved in phosphonates catabolism (phnGHKL) (Hove-Jensen *et al.* 2014). The qPCR primers were specifically designed in this study for the strain *Acidovorax* sp. CNI26 using Primer3Plus (Untergasser *et al.* 2007). The primers used were CP-lyasesF (5'-CCA CCC YTT TGA RGT GCA GC-3') and CP-lyasesR (5'-CCT GGC AAT AGT CSG AG-3') for the C-P lyase gene expression and GlyoxF (5'-CTA CAT CGC GCC CAA ACA AG-3') and GlyoxR (5' ATT GTG TGG CCA GCT CCA G 3') for glycine oxidase expression.

RT-qPCR analysis on glyphosate-degrading genes was performed using total RNA extracted from strain CNI26 exposed to glyphosate, AMPA and K_2HPO_4 as P source in triplicate. RNA samples were taken at the middle and the end of the exponential decay phases of glyphosate (100 and 124 hours) and AMPA (36 and 48 hours) dissipation curves observed in the previous biodegradation experiment. Five millilitres of the CNI26 bacterial culture were quickly sampled from each experimental condition, mixed with RNAlater® solution (1:1 v:v) and stored at 4 °C until RNA extraction. Before RNA extraction, bacteria were washed twice with 1X PBS. Total RNA was extracted according to the method described by Toledo-Arana *et al.* (2009). Briefly, bacteria were mechanically lysed with the PreCellys 24 system (Bertin Technologies, Montigny le Bretonneux, France) at a speed of 6.5 m s^{-1} for two consecutive cycles of 30 s. After acid phenol and TRIzol® extraction, total RNA was precipitated with isopropanol and treated with 10 units of TURBO DNase. After a second phenol-chloroform extraction and ethanol precipitation, RNA pellets were suspended in DEPC-treated water. The efficiency of the DNase treatment was checked by PCR using the 16S BAC338f/515r primers (Borrel *et al.* 2012). RNA concentration in the extracts was quantified with the Qubit system (Thermo Fisher Scientific). Extracted RNA was then converted into cDNA with the SuperScript III Reverse Transcriptase kit (Invitrogen, USA) using Random Primers (Invitrogen) and according to the manufacturer's instructions. qPCR was performed in a CFX96 touch Real-Time PCR detection system (BioRad, USA) using the MESA GREEN qPCR Master Mix Plus kit (Eurogentec) coupled with white qPCR96-well plates (Eurogentec) in a final volume of 15 µL and using the C-P lyase and glycine oxidase primers described above. The qPCR conditions were as follows: initial denaturation at 95 ºC for 5 min, 40

cycles of denaturation at 95 ºC for 30 s, primer annealing at 60 ºC for 15 s and elongation at 72 ºC for 20 s. C-P lyase and glycine oxidase gene expressions were normalized using the 16S rRNA (BAC338f/515r) as the housekeeping gene.

2.5 Data treatment and statistical analyses

Bacterial growth during biodegradation experiments for each of the 5 isolated strains was fitted to the Gompertz growth model (SGompertz) according to the following equation:

$$Bt = Maxe^{-e^{(-mg(x-Max50))}}$$

Where *Bt* is the bacterial density (in cells mL^{-1}) at time *t*, *Max* is the maximum amplitude of the curve (cells mL^{-1}), Max_{50} is the time required (hours) for bacterial density to increase 50 % of the initial value and m_g is the growth rate coefficient ($hours^{-1}$). Direct comparisons between treatments (glyphosate, AMPA) and control (K_2HPO_4) for the Max_{50} parameter was achieved by the ratio Max_{50}_treatment/Max_{50}_control calculation. A ratio value < 1 indicates lower Max_{50} values in the treatment (faster growth) than in the control, whereas a ratio > 1 indicates higher Max_{50} values in the treatment (slower growth) than in the control.

Dissipation kinetics of glyphosate, AMPA and K_2HPO_4 molecules in the media during biodegradation experiments were fitted to a dose-response sigmoidal model (DosResp), according to the following equation:

$$Ct = Cf + \frac{Ci - Cf}{1 + 10^{(DT50-x)md}}$$

where *Ct* is the molecule concentration (µM) at time *t*, *Ci* the initial concentration of the molecule (µM), *Cf* the final concentration of the molecule (µM), DT_{50} the time required to decrease the concentration of the molecule by 50 % of its initial concentration value (hours) and m_d the dissipation rate coefficient ($hours^{-1}$). Direct comparison between treatments (glyphosate and AMPA) and control (K_2HPO_4) for the DT_{50} parameter was achieved by the ratio DT_{50}_treatment/DT_{50}_control calculation. A ratio < 1 indicates lower DT_{50} values in the treatment (faster dissipation) than in the control, whereas a ratio > 1 indicates higher DT_{50} values in the treatment (slower dissipation) than in the control.

All fittings were performed using the OriginPro 2016 software (Origin Lab Corporation, USA).

Statistical differences related to the bacterial growth kinetics parameters (*Max*, Max_{50} and m_g) or glyphosate, AMPA and K_2HPO_4 dissipation kinetics parameters (DT_{50} and m_d) among the five isolated bacterial strains were assessed using multiple Kruskal-Wallis tests followed by separate pairwise comparison tests using the Tukey's contrast. The factors tested were strain (CNII15, CNI26, CNI28, CNI35 and CNI52), P-source (glyphosate, AMPA and K_2HPO_4) and their interaction (strain × P source).

C-P lyase and glyphosate oxidase gene expression was expressed as the relative quantity of copies of genes in each of the P-source treatments (glyphosate, AMPA and K_2HPO_4) following the model of Pfaffl (2001):

$$\text{Relative quantity} = \frac{E^{-CqS1Gi}}{E^{-CqS1GR}}$$

where *E* is the primer efficiency, *CqSiGi* is the threshold cycle for the gene of interest (i.e. C-P lyase or glycine oxidase) and *CqSiGR* is the threshold cycle for the housekeeping gene (16S). Statistical differences between sampling times within glyphosate and AMPA treatments were performed for each gene separately using the Kruskal-Wallis test.

All the statistical analyses were computed using the R software Version 4.0.3 at the alpha threshold of 0.05.

3. RESULTS

3.1 Bacterial growth and taxonomic affiliation

Most of the strains were able to grow in the presence of K_2HPO_4, glyphosate or AMPA as unique P source, except CNII15 in the presence of glyphosate (Table 1, Figure S1). P treatments had a significant effect on the growth dynamics of bacterial strains; the lowest time required to increase bacterial density by 50 % (Max_{50}) was observed with K_2HPO_4 (48.3 ± 5.3 days on average for the 5 strains), followed by AMPA (80.3 ± 21.9 days) and glyphosate (168.1 ± 37.9 days) (Kruskal-Wallis test, $P < 0.001$; Table 2). DT_{50}/DT_{50_K2HPO4} ratio calculations confirmed the same trend; AMPA treatment displayed lower ratio values ranging from 0.95 to 1.49 (except CNII15, ratio = 4.32) compared to the glyphosate treatment ranging from 2.22 to 4.61 (Table 1).

Strain growth also varied within P treatments (Strain × P treatment, Table 2). According to the Max_{50} results, strain CNI28 grew faster in the presence of K_2HPO_4, strains CNI26 and CNI28 grew faster in the presence of AMPA, and finally, strain CNI26 grew faster in the presence of glyphosate (Tukey's test, $P < 0.05$; Table 1). Maximal bacterial density (*Max*) was not different among P treatments ($P = 0.44$), although an interaction effect existed between strains and P treatments (Table 2). Comparatively, the highest *Max* values in the presence of K_2HPO_4, AMPA and glyphosate were observed for strains CNI35, CNII15 and CNI52, respectively (Tukey's test, $P < 0.05$; Table 1). No statistical differences were observed for growth rates (m_g) among P treatments ($P = 0.10$) but strain x P treatment interaction existed for K_2HPO_4 and AMPA ($P < 0.05$ both, Table 2). The highest $m_g$values in the presence of K_2HPO_4 and AMPA were observed for CNI52 and CNI28, respectively (Table 1). The strong variability of m_g values among strains in the presence of glyphosate resulted in non-statistical differences.

Four out of the five isolated strains showed an affiliation with α-proteobacteria: *Ensifer* sp. (CNII15), *Agrobacterium tumefaciens* (CNI28), *Novosphingobium* sp. (CNI35) and *Ochrobactrum pituitosum* (CNI52), whereas only one showed affiliation with β-proteobacteria: *Acidovorax* sp. (CNI26) (Figure 2). The majority of known glyphosate-degrading strains in α- and β-proteobacteria use glyphosate as the source of P, whereas few exceptions use the herbicide as the source of C (*Agrobacterium tumefaciens* P5 and *Achromobacter* sp. CH1, Figure 2).

Figure 2. Phylogenetic analysis of the five bacterial strains isolated from stream biofilms, together with the known bacterial glyphosate-degrading strains based on 16S gene sequence (Table S1). Only one sequence per genus has been included in the present analysis, either the 16S rDNA gene sequence of the glyphosate-degrading strain described, or the sequence of a corresponding genus/species if the degrading strain sequence was not available (NA). The alignment was performed with ClustalW. The tree was constructed with the Neighbor-Joining (N = 1000 bootstrap replicates) using MEGA6. Scale bar = 0.05 substitution per site. Bootstrap percentages ≥ 50 % are indicated near tree nodes. For the glyphosate-degrading strains, the metabolism of glyphosate (source of carbon (C), nitrogen (N) and phosphorus (P)) and the main metabolite (AMPA (A), Sarcosine (S), formaldehyde (F), glycine (G) or unknown (U)) are also indicated on the right.

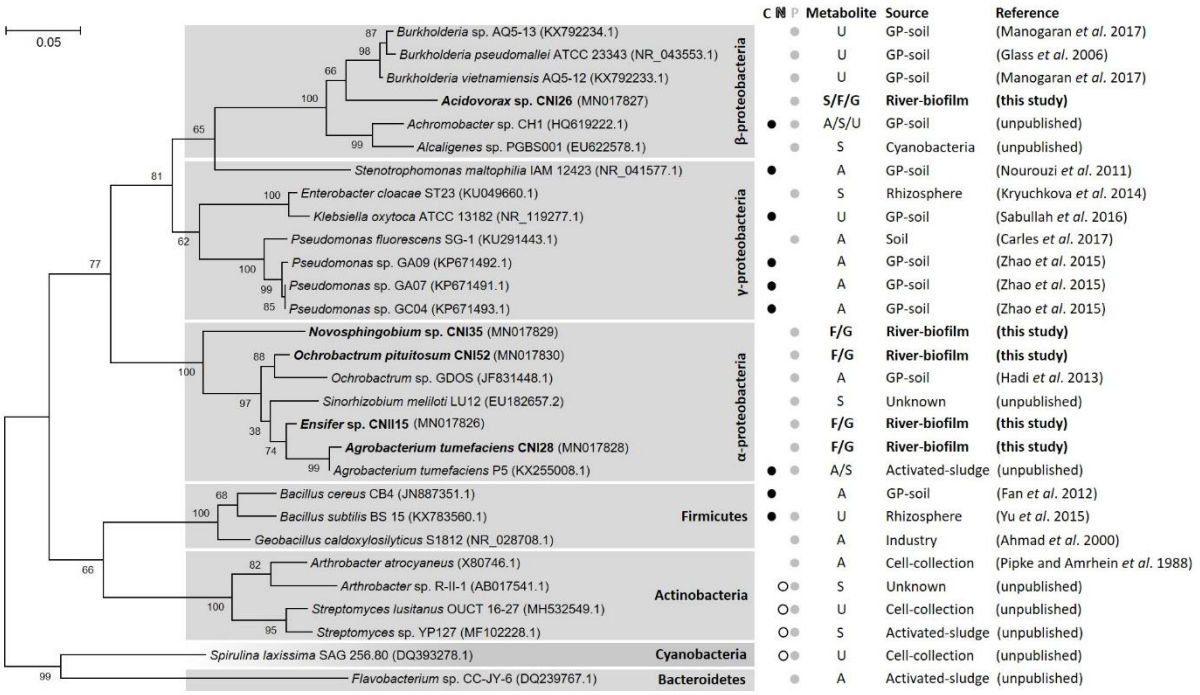

Table 1. Microbial growth estimated parameters (*Max*, Max_{50}, m_g) and model fitting (R-square) are represented for each microbial strain subjected to glyphosate, AMPA and Phosphorus (control) treatments. Pairwise comparisons tests (Tukey's contrast, $P < 0.05$) on growth parameters were run between (uppercase letters) and within (lowercase letters) treatments. N.S means not statistically significant and N.D means that data did not fit the dose-response sigmoidal model.

	Strain	Growth model parameters									
		Max (Cell mL^{-1})			Max_{50} (Hours^{-1})			m_g (Hours^{-1})			R^2	$Max_{50}/Max_{50\_}K_2HPO_4$
K_2HPO_4	CNII15	6.22E8 ± 7.57E7	(b)		38.50 ± 0.13	(d)		0.075 ± 0.003	(c)		0.992 ± 0.002	1
	CNI26	2.00E8 ± 6.21E6	(e)		45.17 ± 0.78	(c)		0.048 ± 0.003	(d)		0.996 ± 0.001	1
	CNI28	4.26E8 ± 3.80E6	(d)		36.79 ± 1.21	(e)	(C)	0.107 ± 0.011	(a)		0.993 ± 0.001	1
	CNI35	6.76E8 ± 1.13E7	(a)		63.97 ± 0.72	(a)		0.088 ± 0.002	(b)		0.954 ± 0.011	1
	CNI52	4.95E8 ± 2.30E7	(b)		57.16 ± 0.39	(b)		0.114 ± 0.013	(ab)		0.867 ± 0.017	1
AMPA	CNII15	6.59E8 ± 1.50E7	(a)		159.11 ± 1.45	(a)		0.037 ± 0.002	(c)		0.992 ± 0.003	4.32 ± 0.02
	CNI26	2.34E8 ± 1.56E6	(d)		42.91 ± 0.30	(d)		0.050 ± 0.002	(b)		0.993 ± 0.001	0.95 ± 0.02
	CNI28	4.20E8 ± 5.59E6	(c)	(N.S)	43.60 ± 0.66	(d)	(B)	0.107 ± 0.011	(a)	(N.S)	0.979 ± 0.006	1.19 ± 0.06
	CNI35	5.14E8 ± 1.14E7	(b)		95.73 ± 1.74	(b)		0.097 ± 0.005	(a)		0.992 ± 0.004	1.49 ± 0.04
	CNI52	5.64E8 ± 3.69E7	(ab)		60.06 ± 0.47	(c)		0.099 ± 0.019	(a)		0.957 ± 0.014	1.05 ± 0.01
Glyphosate	CNII15	N.D			N.D			N.D			N.D	N.D
	CNI26	9.21E7 ± 2.15E6	(c)		116.53 ± 2.62	(c)		0.111 ± 0.017			0.988 ± 0.001	2.58 ± 0.03
	CNI28	3.99E8 ± 4.27E7	(b)		134.58 ± 10.42	(b)	(A)	0.015 ± 0.002	(N.S)		0.973 ± 0.004	3.66 ± 0.24
	CNI35	5.48E8 ± 2.88E7	(ab)		294.58 ± 25.68	(a)		0.066 ± 0.046			0.996 ± 0.002	4.61 ± 0.42
	CNI52	5.59E8 ± 7.70E7	(a)		126.65 ± 2.56	(b)		0.041 ± 0.004			0.981 ± 0.001	2.22 ± 0.06

Table 2. Results of the Kruskal-Wallis tests performed on bacterial growth model parameters (*Max*, Max_{50} and m_g) and dissipation model parameters (DT_{50} and k_d). The tested factors are P treatments (K_2HPO_4, AMPA or glyphosate) and the interaction between strains (CNII15, CNI26, CNI28, CNI35, CNI52) and P treatments. X^2 statistic scores, degrees of freedom (*Df*) and *P-values* were provided for each source of variation. Bold values indicate significant differences at $P < 0.05$.

Kruskal-Wallis		**Dissipation model parameters**						**Growth model paraemters**								
Testedfactors		m_d			DT_{50}			m_q			Max_{50}			*Max*		
		X^2	*Df*	*p value*	X^2	*Df*	*p value*	X^2	*Df*	*p value*	X^2	*Df*	*p value*	X^2	*Df*	*p value*
P source		22.88	2	< **0.001**	22.19	2	< **0.001**	4.54	2	0.10	21.77	2	< **0.001**	1.61	2	0.44
Strain x	K_2HPO_4	12	4	< **0.05**	12.9	4	< **0.05**	12.4	4	< **0.05**	13.5	4	< **0.01**	13.5	4	< **0.01**
	AMPA	12.63	4	< **0.05**	12.9	4	< **0.05**	10.9	4	< **0.05**	13.03	4	< **0.05**	12.7	4	< **0.05**
	Gly	8.64	3	< **0.05**	6.58	3	0.08	6.89	3	0.07	9.35	3	< **0.05**	8.69	3	< **0.05**

3.2 Phosphorus, glyphosate and AMPA dissipation

Initial concentrations in P-equivalents of K_2HPO_4, AMPA and glyphosate averaged 117.1 ± 4.3 µM (C_i) and final concentrations dropped to 0 µM (C_f) for all P treatments and strains (Table 3). Accumulation of glyphosate and/or AMPA in strain biomass at the end of experiments was < 0.5 % of the initial amount of glyphosate and/or AMPA added. All the strains were able to use either of the above-mentioned compounds as sole P source, except CNII15, which was not able to use glyphosate (Figure 3). However, differences in dissipation kinetics between P treatments as well as among strains x P treatments were observed (Table 2). Average DT_{50} values for K_2HPO_4 and AMPA (34.8 ± 5.7 and 67.4 ± 22.1 hours, respectively) were higher compared to that of glyphosate (165.1 ± 46.2 hours; Tukey's test, $P < 0.05$; Table 3). This was confirmed by DT_{50}/DT_{50_K2HPO4} ratio calculations which displayed average ratio values ranging from 1.02 to 1.85 for AMPA and 2.22 to 6.60 for glyphosate. Dissipation rates (m_d) were also higher for K_2HPO_4 (0.53 ± 0.21 hours^{-1}) and AMPA (0.29 ± 0.12 hours^{-1}) compared to glyphosate (0.04 ± 0.01 hours^{-1}) (Tukey's test, $P < 0.05$; Table 3). The CNII15 strain was the only exception for slow AMPA dissipation reaching a DT_{50}/DT_{50_K2HPO4} ratio of 5.12 and m_d of 0.05 ± 0.018 hours^{-1}.

The strain x P treatment interaction on the DT_{50} parameter revealed faster AMPA dissipation by CNI26 and CNI28 strains (Tukey's test, $P < 0.05$) and faster glyphosate dissipation by CNI26 and CNI52 strains, although not statistically significant ($P > 0.05$, Table 3). Dissipation rates (m_d) differed between strains in the same manner that DT_{50} did. For instance, the highest AMPA dissipation rates were found in CNI26 and CNI28 (0.662 and 0.464 hours^{-1}, respectively) while the highest glyphosate dissipation rates were found in CNI26 and CNI52 (0.055 and 0.056 hours^{-1}, respectively) (Tukey's test, $P < 0.05$).

Figure 3. Dissipation kinetics of K_2HPO_4 (A), AMPA (B) and glyphosate (C) for the five bacterial strains (CNII15, CNI26, CNI28, CNI35, CNI52). Fittings to the dose-response sigmoidal model (DosResp) are represented. Lines correspond to the model with mean parameters values for each condition. The values are means ± standard errors (n = 3) of the experimental data.

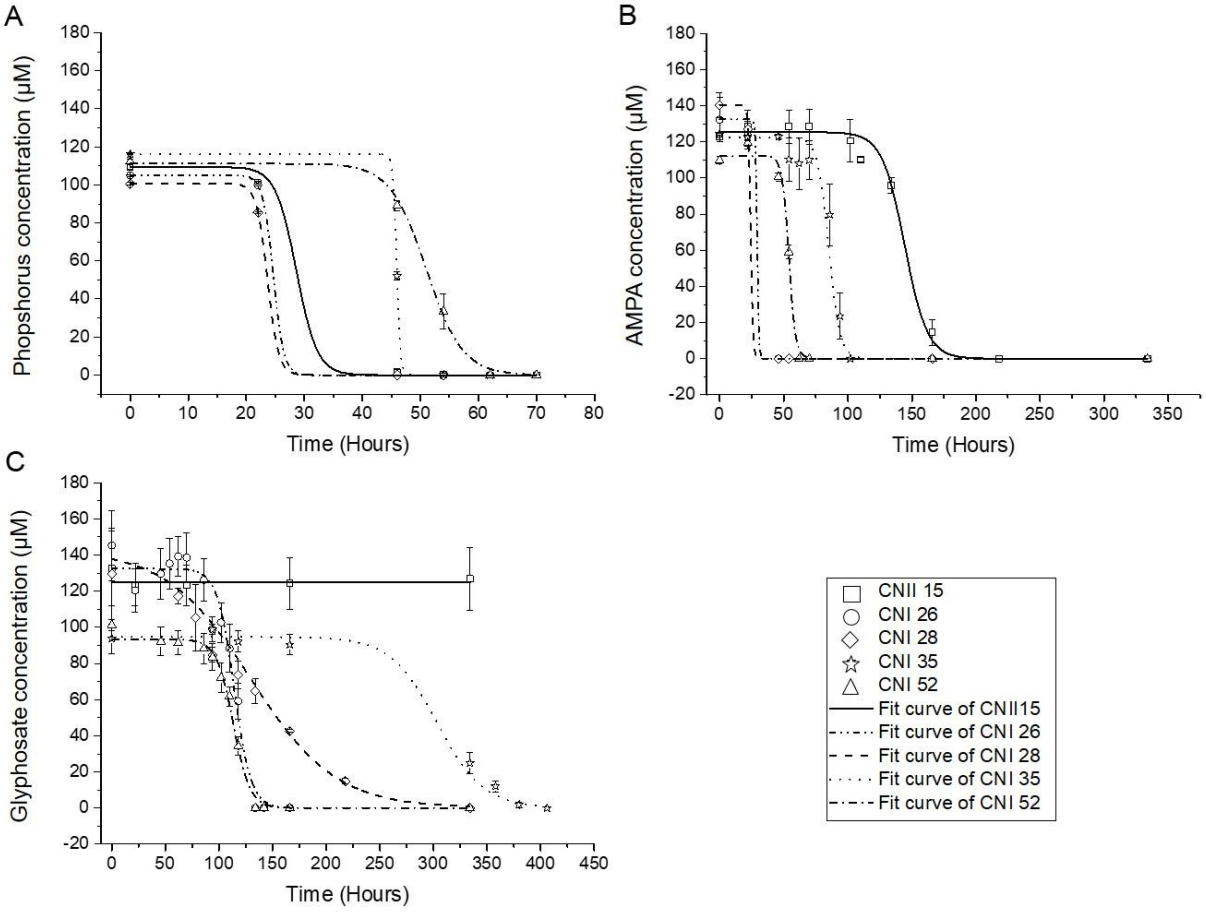

Table 3. Kinetics of K_2HPO_4, AMPA and glyphosate dissipation for each bacterial strain analyzed (CNII15, CNI26, CNI28, CNI35, CNI52). Values of the model parameters are final concentration (*Cf*), initial concentration (*Ci*), dissipation time 50% (DT_{50}), dissipation rate (m_d) and coefficient of determination (R^2) are reported as the mean ± standard error. Statistical differences between P treatments (K_2HPO_4, AMPA or glyphosate) are indicated by the uppercase letters (A > B > C, Tukey's test, $P< 0.05$) whereas statistical differences between strains are indicated by the lowercase letters (a > b > c > d, Tukey's test, P < 0.05). N.S means not statistically significant and N.D: no fittingto dose-response sigmoidal model.

	Strain	Dissipation model parameters									
		Cf (µM)	*Ci* (µM)	DT_{50} (Hours^{-1})			m_d (Hours^{-1})			R^2	DT_{50}/DT_{50} K_2HPO_4
	CNII15	0 ± 0	109.44 ± 1.34	28.64 ± 2.50	(c)		0.242 ± 0.114	(ab)		0.999 ± 0.001	1
	CNI26	0 ± 0	105.01 ± 0.61	24.65 ± 0.02	(c)		0.486 ± 0.003	(c)		1 ± 0	1
K_2HPO_4	CNI28	0 ± 0	100.67 ± 0.70	23.65 ± 0.02	(d)	(B)	0.455 ± 0.002	(b)	(B)	1 ± 0	1
	CNI35	0 ± 0	116.24 ± 0.26	45.93 ± 0.03	(b)		1.342 ± 0.033	(d)		1 ± 0	1
	CNI52	0 ± 0	111.20 ± 2.11	51.03 ± 1.22	(a)		0.139 ± 0.005	(a)		0.994 ± 0.004	1
	CNII15	0 ± 0	125.36 ± 7.71	144.41 ± 1.22	(a)		0.049 ± 0.019	(a)		0.987 ± 0.008	5.12 ± 0.47
	CNI26	0 ± 0	132.55 ± 14.65	29.29 ± 5.17	(d)		0.662 ± 0.196	(c)		0.999 ± 0.001	1.18 ± 0.21
AMPA	CNI28	0 ± 0	140.37 ± 6.93	24.15 ± 0.15	(d)	(B)	0.464 ± 0.005	(c)	(B)	1 ± 0	1.02 ± 0.01
	CNI35	0 ± 0	122.32 ± 0.76	85.16 ± 5.61	(b)		0.099 ± 0.031	(a)		0.972 ± 0.026	1.85 ± 0.12
	CNI52	0 ± 0	112.19 ± 1.43	53.99 ± 0.39	(c)		0.165 ± 0.018	(b)		0.991 ± 0.001	1.06 ± 0.02
	CNII15	N.D	N.D	N.D			N.D			N.D	N.D
	CNI26	0 ± 0	132.40 ± 16.76	114.14 ± 2.89			0.055 ± 0.009	(b)		0.945 ± 0.024	4.63 ± 0.12
Glyphosate	CNI28	0 ± 0	142.96 ± 34.15	129.76 ± 22.53	(N.S)	(A)	0.011 ± 0.001	(a)	(A)	0.952 ± 0.014	5.49 ± 0.96
	CNI35	0 ± 0	94.69 ± 6.19	303.32 ± 18.56			0.020 ± 0.004	(a)		0.989 ± 0.009	6.60 ± 0.40
	CNI52	0 ± 0	93.34 ± 5.85	113.33 ± 1.13			0.056 ± 0.005	(b)		0.985 ± 0.008	2.22 ± 0.04

3.3 Metabolite production

In the glyphosate treatment, no AMPA accumulation was observed but varying concentrations of formaldehyde, glycine and sarcosine were detected depending on the strain tested (Figure 4A). Sarcosine was only detected in strain CNI26 at 19 % and 23 % of mass balance calculations at the intermediate and final sampling times. Accumulation of formaldehyde at intermediate and final sampling times (5.3 % and 14 %, respectively), and glycine in much lower concentrations (2.0 % and 2.4 %, respectively), were also observed in the CNI26 strain. The metabolite production pattern was rather similar among CNI28, CNI35 and CNI52, accumulating more formaldehyde on average (13.8 % on average for the three strains) than glycine (3.2 %) at the final sampling time. As described above, metabolite production was negligible for CNII15 subjected to glyphosate since no dissipation was observed (Figure 4A).

In the AMPA treatment, all AMPA was transformed and few metabolites accumulated at the end of the experiment. Metabolites, mostly formaldehyde, were detected at the final sampling time in CNI15, CNI26 and CNI52 (1.16 % on average for the three strains, Figure 4B), whereas strains CNI28 and CNI35 accumulated both glycine (2.6 %) and formaldehyde (7.8 %) at the final sampling time.

Figure 4. Mass balance of glyphosate and metabolites in the glyphosate (A) and AMPA (B) treatments at initial (0 hours; I), intermediate (1/2 dissipation of glyphosate/AMPA; M) and final (complete dissipation of glyphosate/AMPA; F) times for the five bacterial strains.

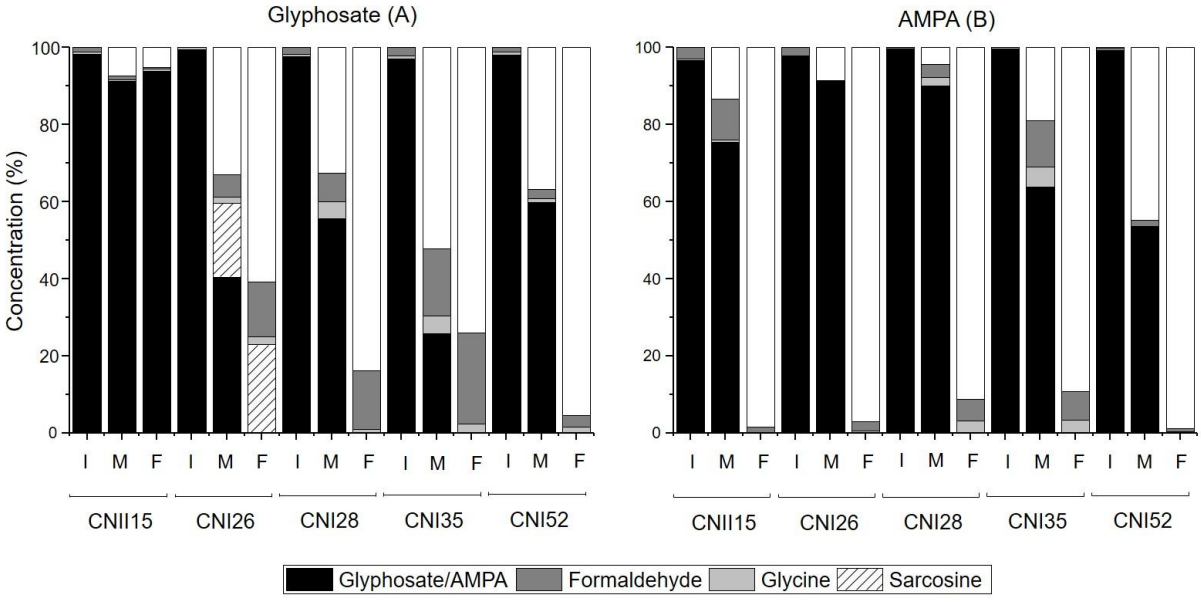

3.4 Glyphosate/AMPA degradation by Acidovorax sp. CNI26

A detailed analysis on metabolite formation by the CNI26 strain subjected to K_2HPO_4 and AMPA treatments revealed stable and quite low concentrations of sarcosine and glycine throughout the experiment (< 10 µM, Figure 5A and B). Formaldehyde concentrations were below the limit of detection regardless of the treatment which contradicts the results obtained in section 3.3, where formaldehyde reached 14 % of mass balance calculations at the final sampling time for CNI26 (Figure 4). In the glyphosate treatment (Figure 5C), sarcosine production was observed along with the dissipation of glyphosate to reach a concentration value of 185 ± 0.6 µM after 168 hours of experiment, close to the initial glyphosate concentration supplied. The sarcosine results coincide with those described in section 3.3 for CNI26 and are in keeping with observations made for known β-proteobacteria glyphosate-degrading strains in the literature (Figure 2).

The relative quantity of C-P lyase and glyphosate oxidase genes (corrected by the 16S rRNA gene) varied among P treatments. Both C-P lyase and the glyphosate oxidase genes increased their expression between 36 h and 48 h in the K_2HPO_4 treatment and between 100 h and 124 h in the glyphosate treatment (Kruskal-Wallis test, $P < 0.05$; Figure 5D and F), although this increase was greater in the presence of glyphosate (30X in average) than in the presence of K_2HPO_4 (10X in average). The opposite trend was observed in the case of the AMPA treatment. The expression of C-P lyase and glyphosate oxidase was overall greater at 36 h than at 48 h, although this difference was only statistically significant for the glyphosate oxidase gene ($P < 0.05$). The expression of C-P lyase at 36 h in the AMPA treatment was extremely variable (Figure 5E).

Figure 5. Kinetics of K_2HPO_4 (A) AMPA (B) or glyphosate (C) dissipation along with metabolites formation (sarcosine, glycine and AMPA) for the CNI26 strain in the culture media exposed to either K_2HPO_4, AMPA or glyphosate. The values are means ± standard errors (n = 3) of the experimental data. The black rectangle highlights the times at which C - P lyases (grey filled) and glycine oxidase (white filled) genes relative quantities were measured in the culture media exposed to either K_2HPO_4 (D), AMPA (E) or glyphosate (F). Asterisks indicate significant differences in genes relative expression (Kruskal-Wallis test, $P< 0.05$).

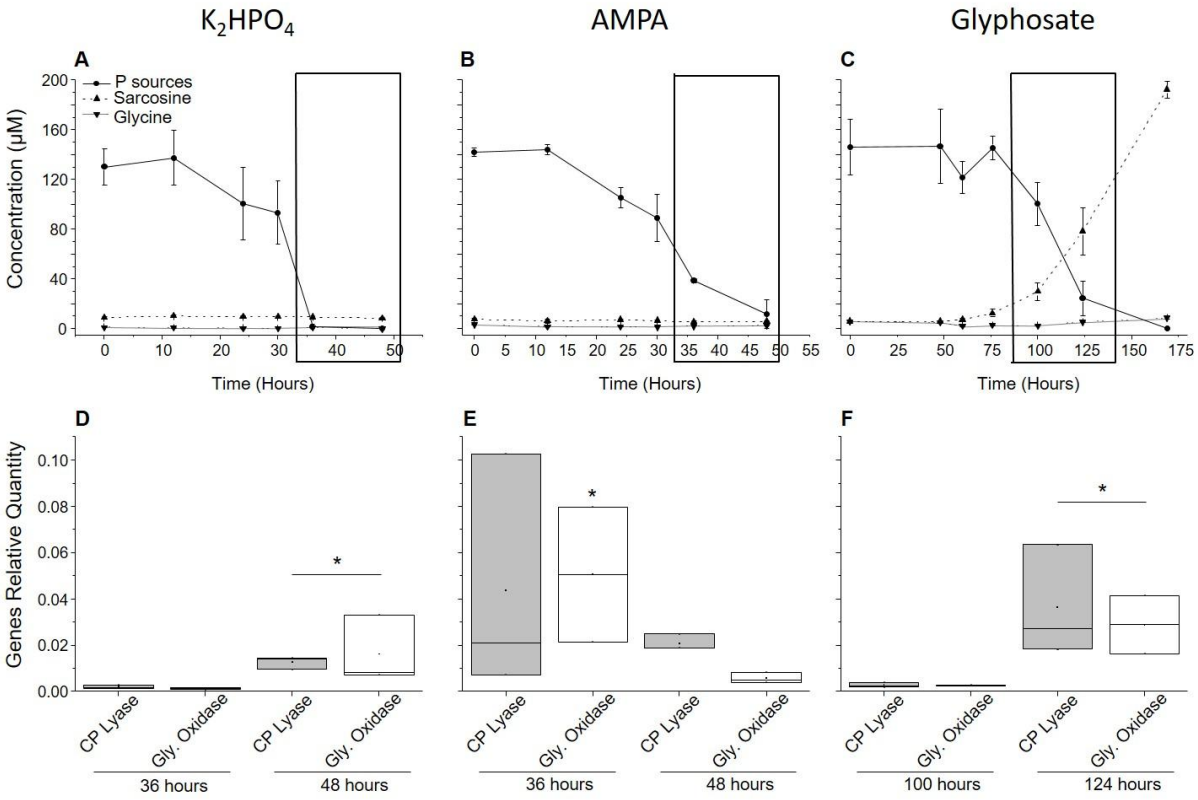

4. DISCUSSION

Four out of the five bacterial strains (*Acidovorax* sp. CNI26, *Agrobacterium tumefaciens* CNI28, *Novosphingobium* sp. CNI35 and *Ochrobactrum pituitosum* CNI52) isolated from stream biofilms were able to completely dissipate AMPA between 30 to 120 hours and glyphosate between 125 to 400 hours when no alternative P source was available. These results are consistent with the literature as the utilization of glyphosate and AMPA as P

sources have been reported as the most common metabolic pathway within bacteria in various environments (including soils, rhizosphere, and industrial effluents or activated sludge; Table S1). For instance, 23 out of 29 strains isolated metabolized glyphosate as P source, against 9 strains as C source and 4 strains as N source (Figure 2). Such generalized use of glyphosate and/or AMPA as P source could be explained by the widespread presence of the C-P lyase enzyme system encoded by the *phn* operon in bacteria (Hove-Jensen *et al*. 2014) which is responsible for C-P bond cleavage and inorganic phosphorus (Pi) transport and assimilation by cells (Chen *et al.* 1990, Stosiek *et al.* 2019). The only exception in our study was strain CNII15 which was not able to degrade glyphosate but completely dissipated AMPA in 200 hours. Indeed, the strain (*Ensifer sp.*CNII15) was neither capable to dissipate nor to grow on glyphosate suggesting: i) lack of adequate enzymatic machinery to metabolize glyphosate despite being able to metabolize AMPA, or ii) slow growth dynamics in the presence of glyphosate within 330 hours. It must be noted that the start of growth for CNII15 in the glyphosate treatment (OD_{600} = 0.18) was observed at 334 hours (Rossi F. personal observation), without glyphosate dissipation, reinforcing the validity of our second hypothesis. When linking the 5 bacterial strains to their environmental origin, four out of the five strains (CNI26, CNI28, CNI35 and CNI52) were isolated from P-poor biofilms from an upstream section of the Artière River, whereas CNII15 was isolated from a P-rich biofilm from the downstream section of the same river (Carles *et al.* 2019). Since the Artière River is characterized by a strong gradient of pesticide contamination between its upstream and downstream sections (including glyphosate and AMPA, Rossi *et al.* 2019), the specific AMPA metabolism of CNII15 may result from site-adaptation mechanisms. For instance, *Ensifer* sp. CNII 15 could benefit from AMPA, which may result from glyphosate biodegradation by other microorganisms in biofilms such as the four other bacterial strains studied.

Dissipation was faster overall for AMPA than for glyphosate as suggested in our initial hypothesis. As expected, the time required for glyphosate/AMPA concentrations to decline 50 % (DT_{50}) was closely related to the time required for the bacterial density to reach 50 % increase (Max_{50}). The AMPA treatment showed lower values of both DT_{50} and Max_{50} compared to the glyphosate treatment. These results are consistent with the literature, since AMPA was already reported as an easier substrate for degradation compared to glyphosate. The review of Hove-Jensen *et al.* (2014) reported that among a total of 133 environmental bacterial strains isolated from glyphosate-treated as well as non-treated soil, 26 strains were able to utilize glyphosate as a P source while 55 strains were capable to use AMPA as P

source. The remaining 52 strains were able to degrade neither glyphosate nor AMPA. Hence, the faster dissipation of AMPA over glyphosate can likely be explained by i) a greater affinity of C-P lyase enzymes for AMPA than glyphosate molecules (Hove-Jensen *et al.* 2014), ii) low affinity of glyphosate oxidase for glyphosate (Pedotti *et al.* 2009), or iii) a purely chemical difference between glyphosate and AMPA, the latter being less complex and consequently being much more easily cleaved to release P. The molecular analysis of *Acidovorax* sp. CNI26 revealed that the highest expression of glycine oxidase and CP-lyase genes was observed before reaching Max_{50} in the presence of AMPA suggesting a decoupling between the expression of these genes and the increase of bacterial density. In contrast, the expression of glycine oxidase and CP-lyase genes was higher after reaching Max_{50} in the presence of glyphosate, hypothesizing that the degrading gene expression and their activity could be linked to the bacterial cell number. Moreover, the faster dissipation of AMPA is favoured by the lower toxicity for aquatic microorganisms of AMPA compared to glyphosate (Bonnet *et al.* 2007).

Differences in AMPA and glyphosate dissipation were observed among the five tested strains. The fastest AMPA dissipation (DT_{50}) was found for CNI26 and CNI28 (29 and 24 hours, respectively), while the fastest dissipation for glyphosate was found for CNI26 and CNI52 (114 and 113 hours, respectively). To our knowledge, our study describes for the first time the ability of the *Acidovorax* genus (*Acidovorax* sp. CNI26) to dissipate both glyphosate and AMPA. The genome sequencing of *Acidovorax* sp. CNI26 revealed the presence of one glycine oxidase gene copy and two copies of the *phn* operon. A study reveals that bacterial glycine oxidase is capable to efficiently cleave glyphosate, producing AMPA and glyoxylate (Pedotti *et al.* 2009). Sviridov *et al.* (2015) speculate that there exists a whole range of bacterial flavin oxidases differing in structure, substrate specificity, and the extent of mutual homology, which can be generically termed glyphosate oxidoreductases (referring to their ability to oxidize glyphosate). Besides, the *phn* operon encodes transport proteins, phosphonate catabolism enzymes and auxiliary polypeptides involved in phosphonate catabolism, among others. Within this operon, seven genes (*phn*G, *phn*H, *phn*I, *phn*J, *phn*K, *phn*L and *phn*M) are supposed to encode the core components of the membrane-bound C-P lyase, metabolizing phosphonates to phosphate by *Phn*J catalyst (Metcalf and Wanner 1993). Both glycine oxidase and *phn*G to M genes confer to *Acidovorax* sp. CNI26 the potential to metabolize glyphosate either through the C-P lyase or the glyphosate oxidase degradation pathways. The genome analysis of several *Agrobacterium* species (including *Agrobacterium vitis* S4, *A. tumefaciens* strain C58, *A. radiobacter* K84) revealed identical *phn* gene orders

conferring the potential to use a variety of phosphonates as P sources (Hove-Jensen *et al.* 2014). Similarly, *Ochrobactrum* species (i. e. *O. anthropi* strain GPK3) phylogenetically close to *Ochrobactrum pituitosum* CNI52 have also been shown able to grow with glyphosate as P source. Both the C-P lyase and the glyphosate oxidase degradation pathways have been suggested for *O. anthropi* strain GPK3 (Sviridov *et al.* 2012). Despite the fact that the genetic potential for successful glyphosate/AMPA degradation seems rather generalized among environmental bacteria, the differences found among bacterial strains could be attributed to a range of factors including differences in i) cellular P requirements and P storage or ii) enzyme affinities and/or catalytic efficiencies for glyphosate and/or AMPA.

Metabolite concentration analyses shed some light on degradation pathways used by bacteria to degrade glyphosate and/or AMPA. On the one hand, the AMPA degradation pathway was similar among all the strains. After complete AMPA dissipation, the five strains accumulated very low concentrations of metabolites, mostly formaldehyde. Also, formaldehyde did not accumulate in the media probably because of incorporation in the microbial biomass via the tetrahydrofolate cycle (Wang *et al.* 2016b). On the other hand, strains CNI28, CNI35 and CNI52 accumulated formaldehyde and glycine after glyphosate transformation. Since no intermediary AMPA or sarcosine metabolites were detected, we can suggest that both C-P lyase and/or glyphosate oxidase degradation pathways could take place. Very low concentrations of easily degradable metabolites are detected at the end of exponential decay phases for glyphosate in CNI28, CNI35 and CNI52 suggesting the incorporation of these metabolites in the microbial biomass or release in the form of CO_2.

The glyphosate degradation pathway was different in the strain *Acidovorax* sp. CNI26, compared to CNI28, CNI35 and CNI52, since it accumulated sarcosine. Sarcosine results from the direct cleavage of the C-P bond by C-P lyases yielding sarcosine and Pi (Figure 1). The detection of this metabolite proves, at least, the existence of the C-P lyase degradation pathway by CNI26 but does not exclude that both the C-P lyase and oxidative pathways were occurring in parallel. This is especially true when comparing the different accumulations of sarcosine and formaldehyde by CNI26 at the end of experiments I and II (see section 3.3 and 3.4). Unfortunately, not all glyphosate/AMPA metabolites were measured in this experiment (glyoxylate and methylamine were missing) to be able to better refine glyphosate/AMPA degradation pathways employed by the different bacterial strains.

The specific analysis of C-P lyase and glycine oxidase genes in *Acidovorax* sp. CNI26 revealed different expression patterns depending on P treatments. The increased expression of C-P lyase and glycine oxidase genes at 124 hours in the glyphosate treatment showed that i)

C-P lyase certainly contributed to sarcosine accumulation in the media and ii) glycine oxidase could contribute to parallel oxidation of sarcosine. Indeed, glycine oxidase from *Bacillus subtilis* (Martínez-Martínez *et al.* 2006) and/or other microbial species (Sviridov *et al.* 2015) has been proven to be capable of oxidative deamination of various amines, including sarcosine. Consequently, the differences in sarcosine accumulation between the first and second experiments suggest that oxidation of sarcosine by glycine oxidase may become relevant in later stages of glyphosate decomposition (Job *et al.* 2002). In the AMPA treatment, expression levels of both C-P lyase and glycine oxidase were high at 36 hours indicating AMPA degradation by C-P lyase as well as methylamine degradation by glycine oxidase. The expression level of these two enzymes decreased at 48 h when neither AMPA nor metabolites remained in the media.

5. CONCLUSION

The present study show that stream biofilms can host bacterial species capable to grow and metabolize both glyphosate and AMPA and other species only capable to metabolize AMPA. The close interactions between microbial species in biofilms are expected to guarantee the survival of species such as *Ensifer sp.* CNII15 tolerant to glyphosate but only able to metabolize AMPA. It must be noted that this study constrained each bacterial strain to use P from glyphosate or AMPA, although other P sources may be available for bacteria in stream biofilms. Hence, glyphosate mitigation by microbial biofilms still depends on P concentration levels in stream waters.

ACKNOWLEDGMENTS

This work was supported by the French National Research Agency in the frame of the BIGLY project (ANR-16-CE32-0001).

REFERENCES

Artigas, J., Batisson, I., Carles, L., 2020. Dissolved organic matter does not promote glyphosate degradation in auto-heterotrophic aquatic microbial communities. Environ. Poll. 259, 113951.

671 Araya, R., Yamaguchi, N., Tani, K., Nasu, M., 2003. Change in the bacterial community of
672 natural river biofilm during biodegradation of aniline-derived compounds determined
673 by denaturing gradient gel electrophoresis. J. Health Sci. 49, 379–385.
674 Batisson, I., Crouzet, O., Besse-Hoggan, P., Sancelme, M., Mangot, J.F., Mallet, C., Bohatier,
675 J., 2009. Isolation and characterization of mesotrione-degrading *Bacillus* sp. from soil.
676 Environ. Pollut. 157, 1195–1201.
677 Battaglin, W.A., Meyer, M.T., Kuivila, K.M., Dietze, J.E., 2014. Glyphosate and its
678 degradation product AMPA occur frequently and widely in US soils, surface water,
679 groundwater, and precipitation. J. Am. Water Resour. Assoc. 50, 275–290.
680 Bazot, S., Lebeau, T., 2008. Simultaneous mineralization of glyphosate and diuron by a
681 consortium of three bacteria as free-and/or immobilized-cells formulations. Appl.
682 Microbiol. Biotechnol. 77, 1351–1358.
683 Benbrook, C. M., 2016. Trends in glyphosate herbicide use in the United States and globally.
684 Environ. Sci. Eur. 28, 1-15.
685 Bhatt, P., Joshi, T., Bhatt, K., Zhang, W., Huang, Y., Chen, S., 2021. Binding interaction of
686 glyphosate with glyphosate oxidoreductase and C–P lyase: Molecular docking and
687 molecular dynamics simulation studies. J. Hazardous Materials 409, 124927.
688 Bonnet, J.L., Bonnemoy, F., Dusser, M., Bohatier, J., 2007. Assessment of the potential
689 toxicity of herbicides and their degradation products to nontarget cells using two
690 microorganisms, the bacteria Vibrio fischeri and the ciliate Tetrahymena pyriformis.
691 Environ. Toxicol. 22, 78–91.
692 Borggaard, O.K., Gimsing, A.L., 2008. Fate of glyphosate in soil and the possibility of
693 leaching to ground and surface waters: a review. Pest Manag. Sci. 64, 441–456.
694 Borrel, G., Lehours, A.C., Crouzet, O., Jézéquel, D., Rockne, K., Kulczak, A., Duffaud, E.,
695 Joblin, K., Fonty, G., 2012. Stratification of Archaea in the Deep Sediments of a
696 Freshwater Meromictic Lake: Vertical Shift from Methanogenic to Uncultured
697 Archaeal Lineages. PLoS ONE 7, 1-14.
698 Carles, L., Gardon, H., Joseph, L., Sanchís, J., Farré, M., Artigas, J., 2019. Meta-analysis of
699 glyphosate contamination in surface waters and dissipation by biofilms. Environ. Int.
700 124, 284–293.
701 Chen, C.M., Ye, Q.Z., Zhu, Z.M., Wanner, B.L., Walsh, C.T., 1990. Molecular biology of
702 carbon-phosphorus bond cleavage. Cloning and sequencing of the phn (psiD) genes
703 involved in alkylphosphonate uptake and C-P lyase activity in Escherichia coli B. J.
704 Biol. Chem. 265, 4461–4471.

Daouk, S., Copin, P.J., Rossi, L., Chevre, N., Pfeifer, H.R., 2013. Dynamics and environmental risk assessment of the herbicide glyphosate and its metabolite AMPA in a small vineyard river of the Lake Geneva catchment. Environ. Toxicol. Chem. 32, 2035–2044.

Directive 2009/128/EC of the European Parliament and of the Council of 21 October 2009 establishing a framework for Community action to achieve the sustainable use of pesticides.

Duke, S.O., Powles, S.B., 2008. Glyphosate: a once-in-a-century herbicide Pest Manag. Sci., 64, 319-325.

Ecophyto II+ (2018) Ministère de la Transition écologique et solidaire. https://agriculture.gouv.fr/le-plan-ecophyto-quest-ce-que-cest. Website visited the 28th August 2020.

Grandcoin, A., Piel, S., Baures, E., 2017. AminoMethylPhosphonic acid (AMPA) in natural waters: Its sources, behavior and environmental fate. Water Res. 117, 187–197.

Horth, H., Blackmore, K., 2009. Survey of glyphosate and AMPA in groundwaters and surface waters in Europe. WRC Rep. No UC8073 2.

Hove-Jensen, B., Zechel, D.L., Jochimsen, B., 2014. Utilization of glyphosate as phosphate source: biochemistry and genetics of bacterial carbon-phosphorus lyase. Microbiol Mol Biol Rev 78, 176–197.

Jacob, G., Garbow, J., Hallas, L., Kimack, N., Kishore, G., Schaefer, J., 1988. Metabolism of Glyphosate in Pseudomonas Sp Strain Lbr. Appl. Environ. Microbiol. 54, 2953–2958.

Job, V., Marcone, G. L., Pilone, M. S., Pollegioni, L., 2002. Glycine oxidase from Bacillus subtilis. Characterization of a new protein. J. Biol. Chem. 277, 6985–6993.

Lamichhane, J.R., Dachbrodt-Saaydeh, S., Kudsk, P., Messéan, A., 2016. Towar a reduced reliance on convetional pesticide in european agriculture. American Phytopatol. Soc. 100, 10-24.

Lawrence, J.R., Kopf, G., Headley, J.V., Neu, T.R., 2001. Sorption and metabolism of selected herbicides in river biofilm communities. Can. J. Microbiol. 47, 634–641.

Maggi, F., la Cecilia, D., Tang, F.H.M., McBrateny, A., 2020. The global environmental hazard of glyphosate use. Sci. Total Environ. 717, 137-167.

Mallat, E., Barceló, D., 1998. Analysis and degradation study of glyphosate and of aminomethylphosphonic acid in natural waters by means of polymeric and ion-exchange solid-phase extraction columns followed by ion chromatography–post-column derivatization with fluorescence detection. J. Chromatogr. A 823, 129–136.

739 Malmqvist, B., Rundle S., 2002. Threats to the running water ecosystems of the world.
740 Environmental Conservation 29, 134–153.
741 Martínez- Martínez, I., Navarro- Fernández, J., Lozada- Ramírez, J.D., García- Carmona, F.
742 and Sánchez- Ferrer, Á., 2006. Maximization of Production of His- Tagged Glycine
743 Oxidase and Its M261 Mutant Proteins. Biotechnol. Progress, 22, 647-652.
744 Mcauliffe, K., Hallas, L., Kulpa, C., 1990. Glyphosate Degradation by Agrobacterium-
745 Radiobacter Isolated from Activated-Sludge. J. Ind. Microbiol. 6, 219–221.
746 Metcalf, W. W., Wanner, B. L., 1993. Evidence for a fourteen-gene, *phn*C to *phn*P locus for
747 phosphonate metabolism in Escherichia coli. Gene 129, 27–32.
748 Meybec, M., 2003. Global analysis of river systems: from Earth system controls to
749 Anthropocene syndromes. Phil. Trans. R. Soc. Lond. B 358, 1935–1955.
750 Meybeck, M., Helmer, R., 1989. The quality of rivers: from pristine stage to global pollution.
751 Palaeogeography, Palaeoclimatology, Palaeoecology (Global and Planetary Change
752 Section) 75, 283–309.
753 Murphy, J., Riley, J., 1962. A modified single solution method for the determination of
754 phosphate in natural waters. Anal. Chim. Acta 27, 31–36.
755 Nowack, B., 2003. Environmental chemistry of phosphonates. Water Res. 37, 2533–2546.
756 Okada, E., Costa, J.L., Bedmar, F., 2016. Adsorption and mobility of glyphosate in different
757 soils under no-till and conventional tillage. Geoderma 263, 78–85.
758 Pedotti, M., Rosini, E., Molla, G., Moschetti, T., Savino, C., Vallone, B., et al., 2009.
759 Glyphosate resistance by engineering the flavoenzyme glycine oxidase. J. Biol.
760 Chem. 284, 36415–36423.
761 Pfaffl, M.W., 2001. A new mathematical model for relative quantification in real-time RT-
762 PCR. Nucleic Acids Res. 29, 45e–445.
763 Pipke, R., Schulz, A., Amrhein, N., 1987. Uptake of glyphosate by an Arthrobacter sp. Appl.
764 Environ. Microbiol. 53, 974–978.
765 Rampazzo, N., Rampazzo Todorovic, G., Mentler, A., Blum, W.E.H., 2013. Adsorption of
766 glyphosate and aminomethylphosphonic acid in soils. Int. Agrophysics 27, 203–209.
767 Rossi, F., Mallet, C., Portelli, C., Donnadieu, F., Bonnemoy, F., Artigas, J., 2019. Stimulation
768 or inhibition: Leaf microbial decomposition in streams subjected to complex chemical
769 contamination, Sci. Total Environ, 648, 1371-1383.
770 Schwarzenbach, R.P., Egli, T., Hofstetter, T.B., von Gunten, U., Wehrli, B., 2010. Global
771 water pollution and human health. Annu. Rev. Environ. Resourc. 35,109-136.

772 Sidoli, P., Baran, N., Angulo-Jaramillo, R., 2016. Glyphosate and AMPA adsorption in soils:
773 laboratory experiments and pedotransfer rules. Environ. Sci. Pollut. Res. 23, 5733–
774 5742.
775 Stosiek, N., Talma, M., Klimek-Ochab, M., 2019. Carbon-Phosphorus Lyase-the State of the
776 Art. Appl. Biochem. Biotechnol. 1–28.
777 Struger, J., Van Stempvoort, D.R., Brown, S.J., 2015. Sources of aminomethylphosphonic
778 acid (AMPA) in urban and rural catchments in Ontario, Canada: Glyphosate or
779 phosphonates in wastewater? Environ. Pollut. 204, 289–297.
780 Studnik, H., Liebsch, S., Forlani, G., Wieczorek, D., Kafarski, P., Lipok, J., 2015. Amino
781 polyphosphonates–chemical features and practical uses, environmental durability and
782 biodegradation. New Biotechnol. 32, 1–6.
783 Sviridov, A.V., Shushkova, T.V., Ermakova, I.T., Ivanova, E.V., Epiktetov, D.O.,
784 Leontievsky, A.A., 2015. Microbial degradation of glyphosate herbicides (Review).
785 Appl. Biochem. Microbiol. 51, 188–195
786 Sviridov, A.V., Shushkova, T.V., Ermakova, I.T., Ivanova, E.V., Leontievsky, A.A., 2014.
787 Glyphosate: safety risks, biodegradation, and bioremediation, in: Current
788 Environmental Issues and Challenges. Springer, pp. 183–195.
789 Sviridov, A.V., Shushkova, T.V., Zelenkova, N.F., Vinokurova, N.G., Morgunov, I.G.,
790 Ermakova, I.T., Leontievsky, A.A., 2012. Distribution of glyphosate and
791 methylphosphonate catabolism systems in soil bacteria Ochrobactrum anthropi and
792 Achromobacter sp. Appl. Microbiol. Biotechnol. 93, 787–796.
793 Talbot, H.W., Johnson, L.M., Munnecke, D.M., 1984. Glyphosate utilization byPseudomonas
794 sp. andAlcaligenes sp. isolated from environmental sources. Curr. Microbiol. 10, 255–
795 259.
796 Tien, C.J., Lin, M.C., Chiu, W.H., Chen, C.S., 2013. Biodegradation of carbamate pesticides
797 by natural river biofilms in different seasons and their effects on biofilm community
798 structure. Environ. Pollut. 179, 95–104.
799 Toledo-Arana, A., Dussurget, O., Nikitas, G., Sesto, N., Guet-Revillet, H., Balestrino, D.,
800 Loh, E., Gripenland, J., Tiensuu, T., Vaitkevicius, K., Barthelemy, M., Vergassola,
801 M., Nahori, M.-A., Soubigou, G., Régnault, B., Coppée, J.-Y., Lecuit, M., Johansson,
802 J., Cossart, P., 2009. The Listeria transcriptional landscape from saprophytism to
803 virulence. Nature 459, 950–956.

804 Untergasser, A., Nijveen, H., Rao, X., Bisseling, T., Geurts, R., Leunissen, J. A. M., 2007.
805 Primer3Plus, an enhanced web interface to Primer3. Nucleic Acids Research 35, 71-
806 74.
807 Vereecken, H., 2005. Mobility and leaching of glyphosate: a review. Pest Manag. Sci.
808 Former. Pestic. Sci. 61, 1139–1151.
809 Vörösmarty, C.J., McIntyre, P.B., Gessner, M.O., Dudgeon, D., Prusevich, A., Green, P.,
810 Glidden, S., Bunn, S.E., Sullivan, C.A., Reidy Liermann C., Davies, P.M., 2010.
811 Global threats to human water security and river biodiversity. Nature 467**,** 555–561.
812 Wang, S., Liu, B., Yuan, D., Ma, J., 2016a. A simple method for the determination of
813 glyphosate and aminomethylphosphonic acid in seawater matrix with high
814 performance liquid chromatography and fluorescence detection. Talanta 161, 700–
815 706.
816 Wang, S., Seiwert, B., Kästner, M., Miltner, A., Schäffer, A., Reemtsma, T., Yang, Q.,
817 Nowak, K.M., 2016b. (Bio)degradation of glyphosate in water-sediment microcosms –
818 A stable isotope co-labeling approach. Water Res. 99, 91–100.
819 Yang, X., Wang, F., Bento, C.P.M., Meng, L., van Dam, R., Mol, H., Liu, G., Ritsema, C.J.,
820 Geissen, V., 2015. Decay characteristics and erosion-related transport of glyphosate in
821 Chinese loess soil under field conditions. Sci. Total Environ. 530–531, 87–95.
822 Zhan, H., Fendg, Y., Fan, X., Chen, S., 2018. Recent advances in glyphosate degradation.
823 Appl. Microbiol. Biotechnol. 102, 5033-5043.
824 Zhang, Q., van der Donk, W.A., 2012. Answers to the carbon–phosphorus lyase conundrum.
825 ChemBioChem 13, 627–629.
826

SUPPLEMENTARY INFORMATION

Figure S1. Bacterial density evolution in K_2HPO_4 (A), AMPA (B) and glyphosate (C) treatments are shown. Lines correspond to fittings to the Gompertz growth model (SGompertz) with mean parameters values for each condition. The values are means ± standard errors (n = 3) of the experimental data.

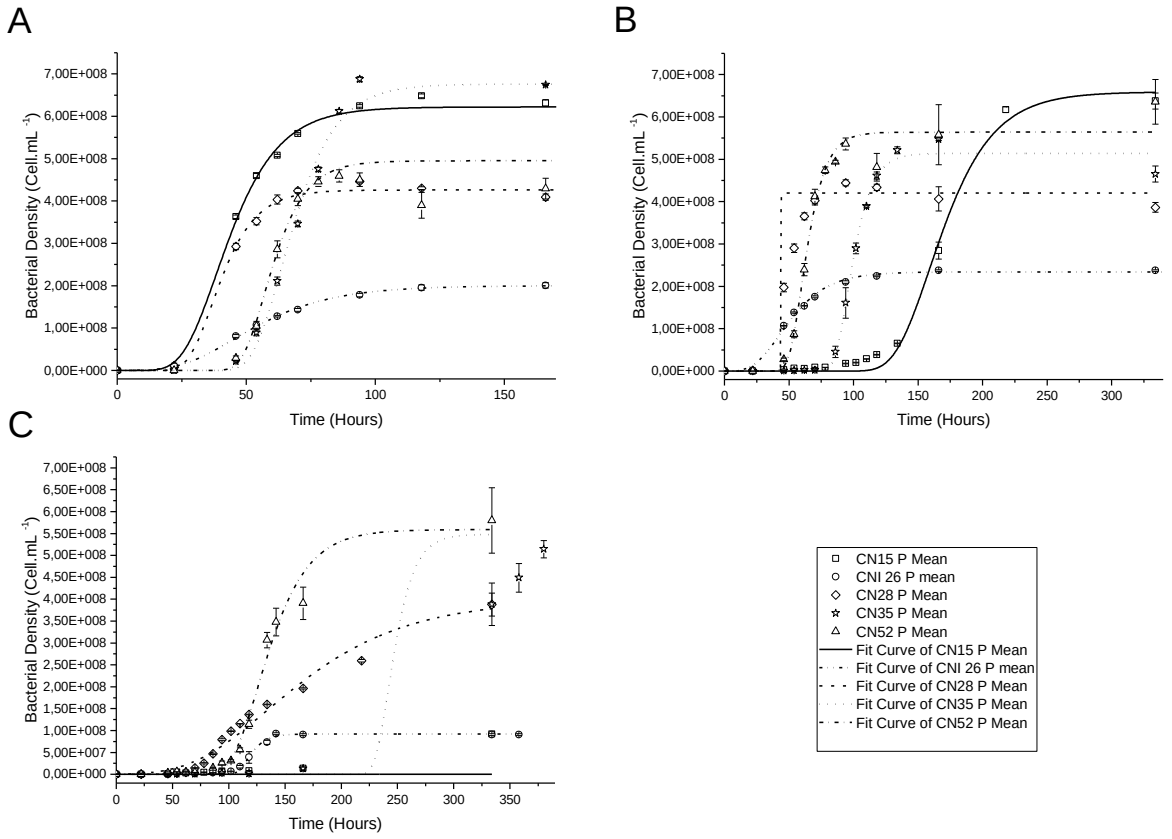

Table S1. Bacterial isolates known for their glyphosate-degrading activity. In addition to the 16S rDNA gene sequences of the 5 newly isolated strains (present study), sequences from previously isolated glyphosate-degrading strains were included in the phylogenetic analysis (Figure 2). These sequences were taken from the studies listed by the review of Sviridov et al. (2015), as well as from more recent studies.

Strain	Source	Metabolite	Metabolism	Reference	NCBI Accession Number	Alternative strain	NCBI Accession Number	Reference
Arthrobacteratrocyaneus ATCC 13752	Cell-collection	AMPA	P	(Pipke and Amrhein, 1988)	X80746.1			
Arthrobactersp. GLP-1	Unknown	Sarcosine	NP	(Pipke et al., 1987)	NA	Arthrobactersp. R-II-1	AB017541.1	Unpublished
Streptomyceslusitanus	Cell-collection	Unknown	NP	(Lipok et al., 2009)	NA	Streptomyceslusitanus strain OUCT 16-27	MH532549.1	Unpublished
Streptomycessp. StC	Activ-sludge	Sarcosine	NP	(Obojska et al., 1999)	NA	Streptomycessp. strain YP127	MF102228.1	Unpublished
Flavobacteriumsp. GD1	Activ-sludge	AMPA	P	(Balthazor and Hallas, 1986)	NA	Flavobacteriumsp. CC-JY-6	DQ239767.1	Unpublished
Spirulinaspp.	Cell-collection	Unknown	NP	(Lipok et al., 2007)	NA	Spirulina laxissima SAG 256.80	DQ393278.1	Unpublished
Bacillus cereus CB4	GP-Soil	AMPA	C	(Fan et al., 2012)	JN887351.1			
Bacillus subtilis Bs-15	Rhizosphere	Unknown	CP	(Yu et al., 2015)	KX783560.1			
Geobacilluscaldoxylosilyticus T20	Industrial	AMPA	P	(Obojska et al., 2002)	NA	Geobacilluscaldoxylosilyticus strain S1812	NR_028708.1	(Ahmad et al., 2000)
Ochrobactrumanthropi GDOS	GP-Soil	AMPA	P	(Hadi et al., 2013)	JF831448.1			
Ochrobactrumanthropi GPK 3	GP-Soil	AMPA	P	(Sviridov et al., 2012)	NA			
Ochrobactrumanthropi LBAA	Soil	AMPA	P	(Gard et al., 1997; Obojska et al., 2002)	NA			
Ochrobactrumanthropi S5	Soil	AMPA	P	(Gard et al., 1997)	NA			
Ochrobactrumpituitosum CNI52	River-biofilm	Unknown	P	This study	MN017830			
Agrobacteriumradiobacter	Activ-sludge	Sarcosine	P	(Wackett et al., 1987)	NA	Agrobacteriumtumefaciens P5	KX255008.1	Unpublished
Agrobacteriumradiobacter SW9	Activ-sludge	AMPA	C	(Mcauliffe et al., 1990)	NA			
Agrobacteriumtumefaciens CNI28	River-biofilm	Unknown	P	This study	MN017828			

Rhizobium meliloti 1021	Unknown	Sarcosine	P	(Liu et al., 1991)	NA	Sinorhizobiummeliloti strain LU12	EU182657.2	Unpublished
Sinorhizobiumsp. CNII15	River-biofilm	Unknown	P	This study	MN017826			
Novosphingobiumsp. CNI35	River-biofilm	Unknown	P	This study	MN017829			
Achromobacter sp. Kg 16	GP-Soil	Unknown	P	(Ermakova et al., 2010; Shushkova et al., 2016)	NA	Achromobacter sp. CH1	HQ619222.1	Unpublished
Achromobacter sp. LW9	Activ-sludge	AMPA	C	(Mcauliffe et al., 1990)	NA			
Achromobacter sp. MPK 7	GP-Soil	Sarcosine	P	(Ermakova et al., 2017)	NA			
Achromobacter sp. MPS 12A	phosphonate-Soil	Sarcosine	P	(Sviridov et al., 2012)	NA			
Alcaligenessp. GL	Cyanobacteria	Sarcosine	P	(Lerbs et al., 1990)	NA	Alcaligenessp. PGBS001	EU622578.1	Unpublished
Burkholderiasp. AQ5-13	GP-Soil	Unknown	P	(Manogaran et al., 2017)	KX792234.1			
Burkholderiavietnamiensis AQ5-12	GP-Soil	Unknown	P	(Manogaran et al., 2017)	KX792233.1			
Acidovoraxsp. CNI26	River-biofilm	Unknown	P	This study	MN017827			
Enterobactercloacae K7	Rhizosphere	Sarcosine	P	(Kryuchkova et al., 2014)	NA	Enterobactercloacae strain ST23	KU049660.1	Unpublished
Klebsiellaoxytoca SAW-5	GP-Soil	Unknown	C	(Sabullah et al., 2016)	NA	Klebsiellaoxytoca strain ATCC 13182	NR_119277.1	(Boye and Hansen, 2003)
Providenciaalcalifaciens	GP-Soil	AMPA	C	(Nourouzi et al., 2011)	NA	Providenciaalcalifaciens strain CI P82.90	NR_042053.1	(Dauga, 2002)
Pseudomonas fluorescens	Soil	AMPA	P	(Zboińska et al., 1992)	NA	Pseudomonas fluorescens strain SG-1	KU291443.1	(Carles et al., 2017)
Pseudomonas pseudomallei 22	GP-Soil	AMPA	P	(Peñaloza-Vazquez et al., 1995)	NA	Burkholderiapseudomallei strain ATCC 23343	NR_043553.1	(Glass et al., 2006)
Pseudomonas putida T5	HC-Soil	Sarcosine	P	(Selvi and Manonmani, 2015)	NA	Pseudomonas putida strain IAM 1236	NR_043424.1	(Anzay et al., 1997)
Pseudomonas sp. 4ASW	GP-Soil	Sarcosine	P	(Dick and Quinn, 1995)	NA			
Pseudomonas sp. GA07	GP-Soil	AMPA	C	(Zhao et al., 2015)	KP671491			
Pseudomonas sp. GA09	GP-Soil	AMPA	C	(Zhao et al., 2015)	KP671492			
Pseudomonas sp. GC04	GP-Soil	AMPA	C	(Zhao et al., 2015)	KP671493			
Pseudomonas sp. GLC11	Unknown	Sarcosine	P	(Selvapandiyan and Bhatnagar, 1994)	NA			

Pseudomonas sp. LBr	Activ-sludge	AMPA	P	(Jacob et al., 1988)	NA			
Pseudomonas sp. PG2982	Unknown	Sarcosine	P	(Moore et al., 1983)	NA			
Pseudomonas sp. SG-1	Activ-sludge	AMPA	P	(Talbot et al., 1984)	NA			
Stenotrophomonasmaltophilia	GP-Soil	AMPA	C	(Nourouzi et al., 2011)	NA	Stenotrophomonasmaltophilia strain IAM 12423	NR_041577.1	Unpublished

841